© 2025 THE BIOPHYSICAL SOCIETY OF JAPAN
Vol. 22, e220009 (2025)
doi: 10.2142/biophysico.bppb-v22.0009

Biophysics and Physicobiology
https://www.jstage.jst.go.jp/browse/biophysico/

Regular Article

Structure-activity relationship of PET-degrading cutinase regulated by weak Ca^{2+} binding and temperature

Fumiya Kondo[1], Narutoshi Kamiya[2], Gert-Jan Bekker[3], Satoshi Nagao[4], Nobutaka Numoto[5,6], Hiroshi Sekiguchi[4], Nobutoshi Ito[5], Masayuki Oda[1]

[1] *Graduate School of Life and Environmental Sciences, Kyoto Prefectural University, Kyoto 606-8522, Japan*
[2] *Graduate School of Information Science, University of Hyogo, Kobe, Hyogo 650-0047, Japan*
[3] *Institute for Protein Research, Osaka University, Suita, Osaka 565-0871, Japan*
[4] *Center for Synchrotron Radiation Research, Japan Synchrotron Radiation Research Institute, Hyogo 679-5198, Japan*
[5] *Medical Research Laboratory, Institute of Integrated Research, Institute of Science Tokyo, Tokyo 113-8510, Japan*
[6] *International Center for Structural Biology, Research Institute for Interdisciplinary Science, Okayama University, Okayama 700-8530, Japan*

Received March 10, 2025; Accepted April 22, 2025;
Released online in J-STAGE as advance publication April 24, 2025
Edited by Daisuke Kohda

Enzyme function is often regulated by weak metal-ion binding, which results from conformational changes while maintaining conformational fluctuations. We analyzed the structure and function of cutinase-like enzyme, Cut190, using biophysical methods such as X-ray crystallography and molecular dynamics (MD) simulations, showing that its structure and function are finely regulated by weak Ca^{2+} binding and release. We succeeded to stabilize the enzyme by introducing a disulfide-bond which can degrade polyethylene terephthalate (PET) to PET monomers at the glass transition temperature of PET, ≈ 70°C. In this study, using the stabilized Cut190 mutants, Cut190SS and Cut190**SS_F77L, we evaluated the requirement of Ca^{2+} for catalytic activity at 70°C, showing that the enzyme expressed the activity even in the absence of Ca^{2+}, in contrast to that at 37°C. These results were supported by multicanonical MD analysis, which showed that the respective forms of the enzyme, such as closed, open, and engaged forms, were exchangeable, possibly because the potential energy barriers between the respective forms were lowered. Taken together, the conformational equilibrium to express the catalytic activity was regulated by weak Ca^{2+} binding at 37°C, and was also regulated by increasing temperature. The respective conformational states of Cut190**SS and Cut190**SS_F77L correlated well with their different catalytic activities for PET.**

Key words: catalytic activity, conformational change, enzyme, multicanonical molecular dynamics simulations, weak metal-ion binding

Significance

Weak Ca^{2+} binding to cutinase-like enzyme, Cut190, induces its conformational change and expresses its activity. The stabilized mutants of Cut190 by introduction of a disulfide-bond can degrade polyethylene terephthalate (PET) at 70°C. These mutants expressed the activity at 70°C even in the absence of Ca^{2+}, in contrast to that at 37°C. Multicanonical molecular dynamics simulations showed that the respective conformational states of mutants were exchangeable with increasing temperature, possibly because the potential energy barriers between the respective forms were lowered. The respective states of Cut190 mutants correlated well with their catalytic activities for PET.

Corresponding author: Masayuki Oda, Graduate School of Life and Environmental Sciences, Kyoto Prefectural University, Kyoto 606-8522, Japan. ORCID iD: https://orcid.org/0000-0002-8568-4223, e-mail: oda@kpu.ac.jp

Introduction

Cutinases belong to the lipase superfamily and catalyze the hydrolysis of complex plant biopolymers in the cuticle layer of leaves (cutin) and in the suberin layer of roots (suberin) [1]. A putative cutinase gene (cut190) was cloned from the thermophilic *Saccharomonospora viridis* AHK190, and its protein, Cut190, was expressed in *Escherichia coli* [2]. The catalytic triad of Cut190, Ser176-Asp222-His254, forms an active site (Fig. 1, note that Ser176 was substituted to Ala). A unique feature of Cut190 is that its function is regulated via Ca^{2+} binding. Our crystal structure analyses using Cut190 mutants showed that the closed form underwent an accelerated conformational change to the open form upon Ca^{2+} binding for substrate binding, followed by a change to the engaged form with Ca^{2+} release for substrate hydrolysis [3-6]. In the open form, Phe77 is oriented outwards, and Phe81 is oriented inward, contributing to the hydrophobic core (Fig. 1). In the closed and engaged forms, Phe81 is oriented outwards, and Phe77 is oriented inward, contributing to the hydrophobic core. In the engaged form, Thr107 at the active site moves to form hydrogen bonds with the substrate. These crystal structures indicated that Ca^{2+} binding changed the Cut190 conformation or population, which was closely correlated with its catalytic function. Ca^{2+} plays an important role in maintaining the balance between the open and engaged/closed forms of Cut190. As observed with the native mass spectrometry results [4], our crystal structures also indicated that the three Ca^{2+} ions were bound at Sites 1-3 of Cut190 (Fig. 1). Mutational analyses of the functional roles of three Ca^{2+} binding sites indicated that Sites 1 and 2 were related to activation and thermostabilization, respectively, and Site 3 was supplementally related to both activation and thermostabilization [7]. It should also be noted that Ca^{2+} binding is weaker than that of other metal-ions such as Zn^{2+} and Mn^{2+} [8]. Zn^{2+} binding was observed in isothermal titration calorimetry (ITC) experiments, and the binding stoichiometry 3 was in good agreement with the three binding sites. In contrast, Ca^{2+} binding was below the ITC detection limit [8]. The weak binder, Ca^{2+}, would be essential for the conformational change of Cut190, which is required for catalytic activity [9].

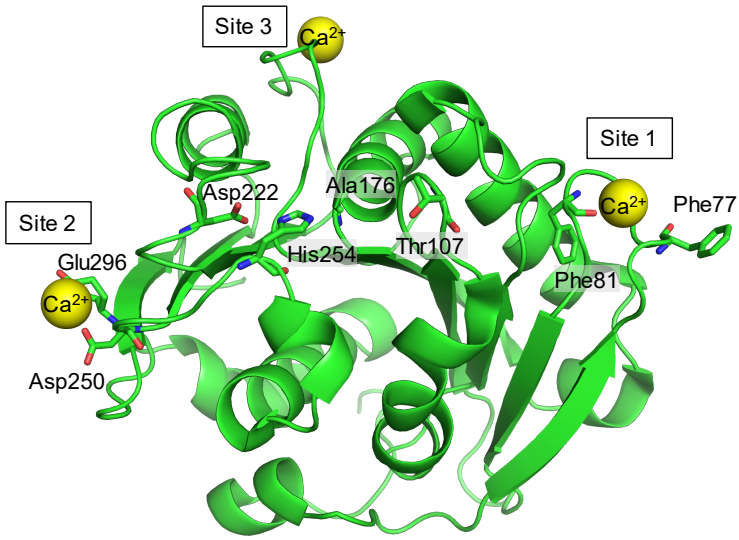

Figure 1 Crystal structure of inactive mutant of Cut190, Cut190*_S176A, in Ca^{2+}-bound state (PDB ID: 5ZNO). The key residues are indicated by stick models. Figure was prepared using the PYMOL software (https://www.pymol.org/).

Thermostable cutinases can be used to chemically recycle polyethylene terephthalate (PET) [10-12]. The depolymerization of PET by an enzyme is one of the most efficient methods, because of its low energy consumption compared with conventional processes using supercritical fluids. In order to depolymerize PET, a thermally stable enzyme is required, because depolymerization of the inner block of PET occurs above the glass transition temperature (T_g), ≈ 70°C. We generated Cut190 mutants to increase stability using S226P/R228S mutant (Cut190*) as a template, and showed that the introduction of a disulfide-bond at Site 2 upon D250C and E296C mutations could significantly increase thermal stability while maintaining its activity [7]. In combination with other mutations to increase both stability and activity [5,7], we succeeded in generating the mutant, Q123H/Q138A/N202H/S226P/R228S/D250C-E296C/K305del/L306del/N307del, designated Cut190**SS, which could depolymerize PET with high efficiency. Furthermore, we found that F77L mutation in Cut190**SS increased its catalytic activity [13].

We evaluated the catalytic activity of Cut190 mutants with high thermal stability at high temperatures. With increasing temperature, the structural dynamics of Cut190 mutants may change, possibly changing the Ca^{2+}-dependent activity. Understanding the mechanism will apply for PET depolymerization and recycling. Using the stabilized Cut190 mutants, Cut190**SS and Cut190**SS_F77L, we could analyze the catalytic activities at 70°C and the correlation with their

conformational states and structural dynamics. In this study, we first analyzed the metal-ion binding of Cut190**SS and Cut190**SS_F77L using ITC. These results support the notion that the metal-ion binding affinity decreased upon the introduction of a disulfide-bond, as observed in Cut190*SS reported previously [6]. However, the catalytic activity of poly(butylene succinate-co-adipate) (PBSA) at 37°C indicated that Ca^{2+} binding is required for activity. In contrast, we found that Cut190**SS and Cut190**SS_F77L expressed catalytic activities towards both PBSA and PET at 70°C even in the absence of Ca^{2+}. This could be explained by the change in the conformational states of the enzyme with increasing temperature, as analyzed using multicanonical molecular dynamics simulations (McMD), which is a generalized ensemble method [14]. With McMD, the bias is correlated with the temperature, enabling McMD simulations to adaptively modulate the bias, given the density of states. Thus, the potential energy surface functions as a reaction coordinate that does not depend on prior knowledge (e.g., any specific conformation). A canonical ensemble at any given temperature, which is a physico-chemically acceptable ensemble, can be generated from a multicanonical ensemble using a reweighting procedure. The free energy landscape (FEL), which governs the thermodynamic properties of a system, can be obtained by mapping the reweighted structural ensemble onto a reaction coordinate, such as a binding path, or onto one or more principal components obtained through Principal Component Analysis (PCA) [15,16]. Analysis of the FEL uncovers stable conformations, as sampled by McMD simulations. Furthermore, analysis of stable structures can provide insight into the conformational preferences of complex molecules [13,17-19]. Thus, these results indicated that catalytic activity is closely correlated with the population of the conformational states that are regulated by Ca^{2+} to overcome the potential energy barriers. With increasing temperature, the energy barriers decreased, enabling the exchange of the respective states without Ca^{2+} binding.

Materials and methods

Proteins

The gene for Cut190**SS was constructed from Cut190*SS. Three residues at C-terminus of Cut190*SS, Lys305-Leu306-Asn307, were removed by introducing a stop codon. The gene for Cut190**SS_F77L was constructed from Cut190**SS by site-directed mutagenesis [13]. The proteins were overexpressed in *Escherichia coli* and purified as reported previously [4]. The protein concentration was spectrophotometrically determined using a molar absorption coefficient of 4.02×10^4 M^{-1} cm^{-1} at 280 nm.

Small-angle X-ray scattering with size-exclusion chromatography (SEC-SAXS) measurements

The SEC-SAXS experiments were performed in two different days (noted as exp. 1 and 2) at BL38B1 of SPring-8 at 20°C, as described previously [20]. The enzyme solution (8.0 mg mL^{-1}), 200 µL, was injected into a Superdex 200 increase 10/300 column (Cytiva) operated by an HPLC system (Shimadzu, Kyoto, Japan) with an elution buffer, 20 mM Tris-HCl pH 7.5, 100 mM NaCl containing 3% glycerol at a flow rate of 0.3 mL min^{-1} (exp. 1) or 0.45 mL min^{-1} (exp. 2). For only Cut190**SS bound to Ca^{2+} (exp. 1), 2.5 mM $CaCl_2$ was included in the elution buffer. The 2D images were processed to obtain 1D scattering profiles with the SAngler (v2.1.65 (exp. 1) and v2.1.68 (exp. 2)) program [21]. The SEC-SAXS data were analyzed with the MOLASS (v1.0.13) program [22]. The range of the magnitude of the scattering vector q used for the SAXS analysis was $0.007 < q\ (=4\pi\sin\theta/\lambda) < 0.43$ $Å^{-1}$, where θ is a half of the scattering angle and λ is the wavelength of X-rays (1.00 Å). The sample-to-detector distance was 2569 nm (exp. 1) or 2390 mm (exp. 2). The scattering curves were calculated with GNOM (v5.0) [23] programs in the ATSAS (v3.2.1) suite [24].

ITC measurements

ITC experiments were carried out at 25°C using iTC200 (Malvern). All samples were in 10 mM Tris-HCl (pH 8.0). A solution of metal-ion (1 mM) was titrated into the enzyme solution (0.03 mM). Each titration consisted of a preliminary 0.5-µL injection followed by subsequent 2-µL additions, which were performed over 5 sec periods at 120 sec intervals. Data were analyzed with the Origin software supplied by MicroCal.

Enzymatic activity measurements

The enzymatic activities for PBSA were measured by monitoring the decrease in the turbidity of PBSA suspension (Bionolle™ EM-301; molecular weight average 1.0×10^5) at 600 nm, as described previously [2]. The reaction mixture including PBSA (8.75 µM, $OD_{600} = 3.5$) and the enzyme (1.33 µM) was incubated at 37°C or 70°C for 30 min with gentle shaking in a water bath. Kinetic values were calculated from Michaelis-Menten plots for degradation of PBSA (3.75 µM to 23.75 µM). The measurements were performed in triplicate.

The enzymatic activities for PET were measured by monitoring the products by reverse-phased HPLC. Amorphous PET (PET-GF, GoodFellow) was homogenized to small particles with a diameter between 30-50 µm. These PET particles, 20 mg, were suspended in a 0.4 mL solution containing 50 mM Tris-HCl (pH 8.7), 2.5 mM $CaCl_2$, and were hydrolyzed by the enzyme, with a final concentration of 0.04 mg/mL, at 70°C for 2 or 24 h. To prevent precipitation of PET particles,

the reaction was carried out with shaking. The hydrolyzed PET monomers, terephthalic acid (TPA), MHET, and bis(2-hydroxyethyl) terephthalate (BHET), were analyzed using a reverse-phased HPLC column, YMC-Pack ODS-AM. The products were eluted using a solvent of 19% acetonitrile containing 0.1% trifluoroacetic acid isocratically, and were monitored by measuring absorbance at 240 nm.

McMD simulations

McMD simulations were conducted to explore the conformational space of cutinase in the presence of bound PET trimer under three different conditions, Ca^{2+}-free Cut190**SS, Ca^{2+}-bound Cut190**SS, and Ca^{2+}-free Cut190**SS_F77L [13]. A multicanonical ensemble was obtained for each system, spanning a temperature range from 280 K to 700 K. To facilitate enhanced local conformational sampling while preventing unfolding, weak distance restraints were applied to the cutinase molecule. These restraints targeted the backbone oxygen and nitrogen atoms for helical and β-sheet secondary structure elements. In addition, distance restraints between selected Cα atoms were added (Glu47-Arg278, Arg48-Glu91, Glu58-Lys263). A repulsive restraint was also introduced for the CBH-CAQ atoms of the PET-trimer to prevent the curling of the PET residues. The conformations were analyzed in a similar manner as our McMD-based dynamic docking simulations [18]. PCA was performed on the loops of β1-β2 (77-81), β4-α3 (105-112), and β3-α2 (131-137) and their surrounding regions using a merged trajectory from the three datasets. For each residue, two atoms were selected; the Cα atom and one representative atom from the sidechain, except for glycine, where only the Cα atom was selected). Atom-pairs were formed between all selected atoms from the loop-selection i versus all selected atoms from the whole enzyme j. Then, atom pairs corresponding to sequential residues ($i \pm 3$ residues) were removed, as were atom pairs whose distance was more than 8 Å in the reference structure (PDB ID: 8Z2I) for atoms j that were not also part of the loop regions. In total, 746 atom pairs were used for the PCA. The structures are then projected onto the first two principal components, and the probability of each bin k on the landscape is calculated as $P_k = \sum_l P_c(E_l)$ using each structure l within bin k, where P_c is the canonical distribution at any given temperature T and E_l is the potential energy of structure l. The free energy as the Potential of Mean Force (PMF) was calculated as $PMF_k = -RTln\ P_k$ for each bin, yielding the 2D free energy landscape (FEL) with the minimum normalized to zero. Here, R is the gas constant and T (= 300 K or 340 K) is the reweighted temperature.

Results

Both Cut190**SS and Cut190**SS_F77L were purified well in their monomeric states (Figs. 2A and S1A). In order to evaluate the conformational states of these enzymes and the effects of Ca^{2+} binding in solution, SEC-SAXS analysis was carried out (Figs. 2 and S1). Kratky plots showed no significant changes in the structures of these enzymes and Cut190**SS due to Ca^{2+} binding. The radii of gyration (R_g) determined from the Gunier plots are summarized in Table 1. These results suggest that the conformational differences in these enzymes and Cut190**SS upon Ca^{2+} binding were below the detection limit of SAXS.

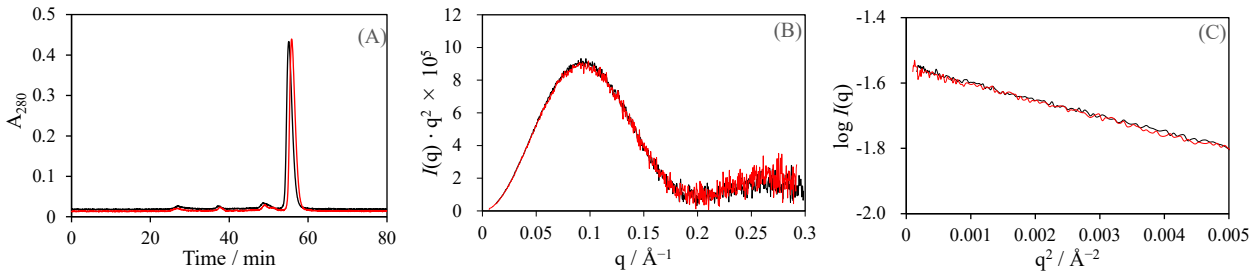

Figure 2 SEC-SAXS analysis (exp. 1). SEC profiles of Cut190**SS in the absence (black line) or presence (red line) of Ca^{2+} (A). The absorbance at 280 nm was recorded using a QEpro UV-visible spectrometer. Kratky (B) and Guinier (C) plots for Cut190**SS in the absence (black line) or presence (red line) of Ca^{2+}.

Metal-ion binding to Cut190**SS and Cut190**SS_F77L was analyzed using ITC, which showed little heat (Fig. 3). This is similar to Zn^{2+} binding to Cut190*SS and Cut190*SS_S176A [6], but not to Cut190*S176A [8]. Thus, the introduction of a disulfide-bond in Cut190 reduced the metal-ion binding affinity below the detection limit of ITC. The introduction of a disulfide-bond at Site 2 also affected the metal-ion binding to Sites 1 and 3. Ca^{2+} binding to Cut190**SS and Cut190**SS_F77L was too low to be detected by ITC (Fig. 3), similar to the previous results for Cut190 mutants

with and without the disulfide-bond [6,8]. The catalytic activities of Cut190**SS and Cut190**SS_F77L at 37°C was activated in the presence of Ca^{2+} (Fig. 4), similar to Cut190*SS [6]. These results indicate that Ca^{2+} specifically binds to the enzyme with a low binding affinity below the ITC detection limit. In comparison with Cut190**, both K_m and k_{cat} values of Cut190**SS decreased, resulting in k_{cat}/K_m that almost unchanged upon the introduction of a disulfide-bond (Table 2). Further mutation of F77L resulted in an increase in the values of both k_{cat} and K_m (Table 2). The catalytic activity towards PBSA at 70°C was also analyzed. In the presence of Ca^{2+}, the activity at 70°C was higher than that at 37°C. Using the stabilized mutants, Cut190**SS and Cut190**SS_F77L,

Table 1 Structural parameters from SEC-SAXS

analyte	R_g, Guinier (Å)
Cut190**SS [a]	18.6 ± 0.06
Cut190**SS + Ca^{2+} [a]	18.6 ± 0.07
Cut190**SS [b]	18.5 ± 0.06
Cut190**SS_F77L [b]	18.5 ± 0.08

[a] exp. 1 (Fig. 2)
[b] exp. 2 (Fig. S1)

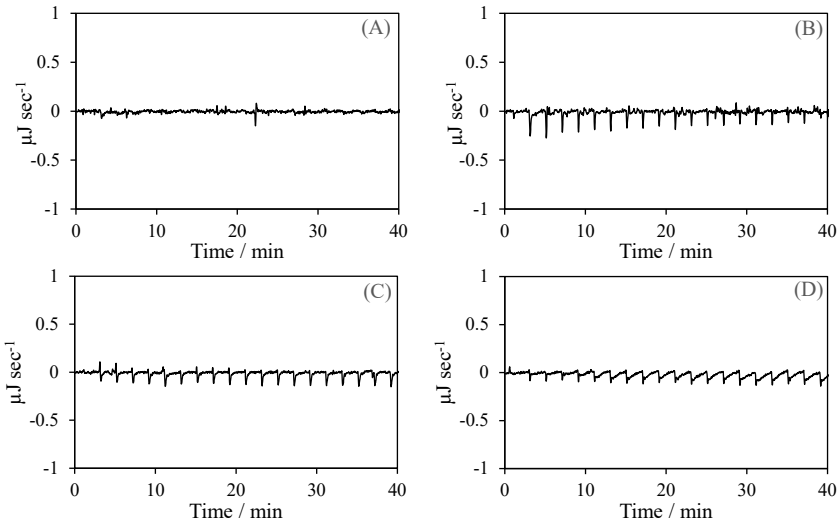

Figure 3 ITC profiles of metal-ion binding to Cut190**SS (A, B) and Cut190**SS_F77L (C, D). Metal ions injected are $ZnCl_2$ (A, C), and $CaCl_2$ (B, D).

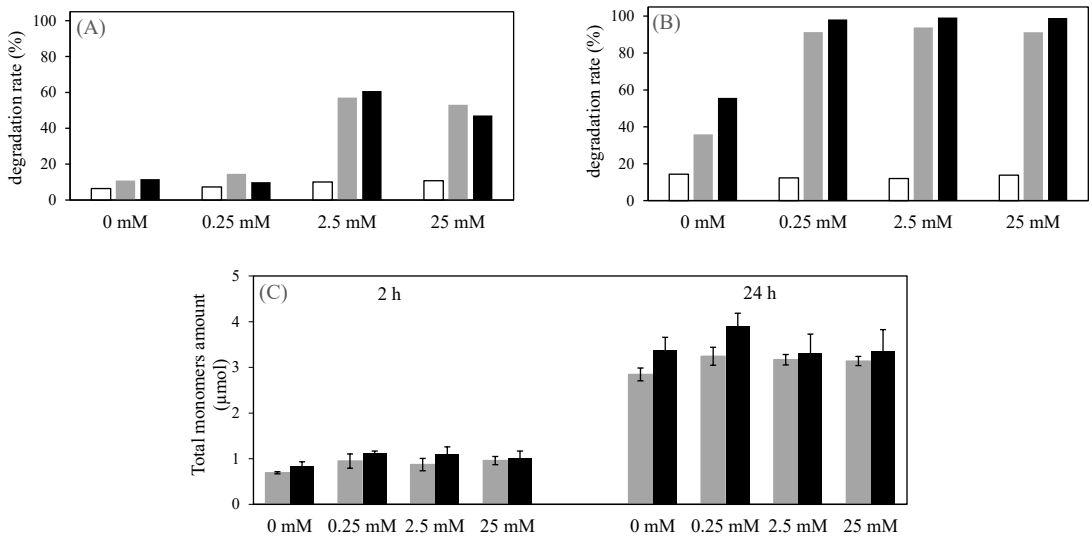

Figure 4 Catalytic activities of Cut190**SS and Cut190**SS_F77L. PBSA degradation by Cut190**SS (gray bar) and Cut190**SS_F77L (black bar) in the absence or presence of Ca^{2+} at 37°C (A) and 70°C (B). The Ca^{2+} concentrations are indicated. The control values for the solution without enzyme are also indicated (white bar). PET degradation by Cut190**SS (gray bar) and Cut190**SS_F77L (black bar) in the absence or presence of Ca^{2+} at 70°C (C). The Ca^{2+} concentrations and the reaction times are indicated. The SD values of triplicate measurements are also indicated.

Table 2 Kinetic parameters of Cut190**SS and Cut190**SS_F77L towards PBSA at 37°C

Enzyme	K_m (mM)	k_{cat} (s^{-1})	k_{cat}/K_m (mM^{-1} s^{-1})
Cut190**SS	0.082	24.9	322
Cut190**SS_F77L	0.215	61.7	277
Cut190*SS [a]	0.079	26.7	327
Cut190** [b]	0.282	100	357

Values averaged from three experiments. The concentration of Ca^{2+} in the reaction mixture was 2.5 mM.
[a] Data were taken from [6].
[b] Data were taken from [5].

it was possible to analyze PET degradation at the glass transition temperature. Notably, even in the absence of Ca^{2+}, activity at 70°C for both PBSA and PET was observed (Fig. 4). For PBSA degradation at 70°C, the activity in the absence of Ca^{2+} was 36% and 56% for Cut190**SS and Cut190**SS_F77L, respectively, and increased up to approximately 100% in the presence of Ca^{2+}. In contrast, for PBSA degradation at 37°C, the activity in the absence or presence of 0.25 mM Ca^{2+} was similar to the control level without the enzyme. For PET degradation at 70°C, the activity in the absence

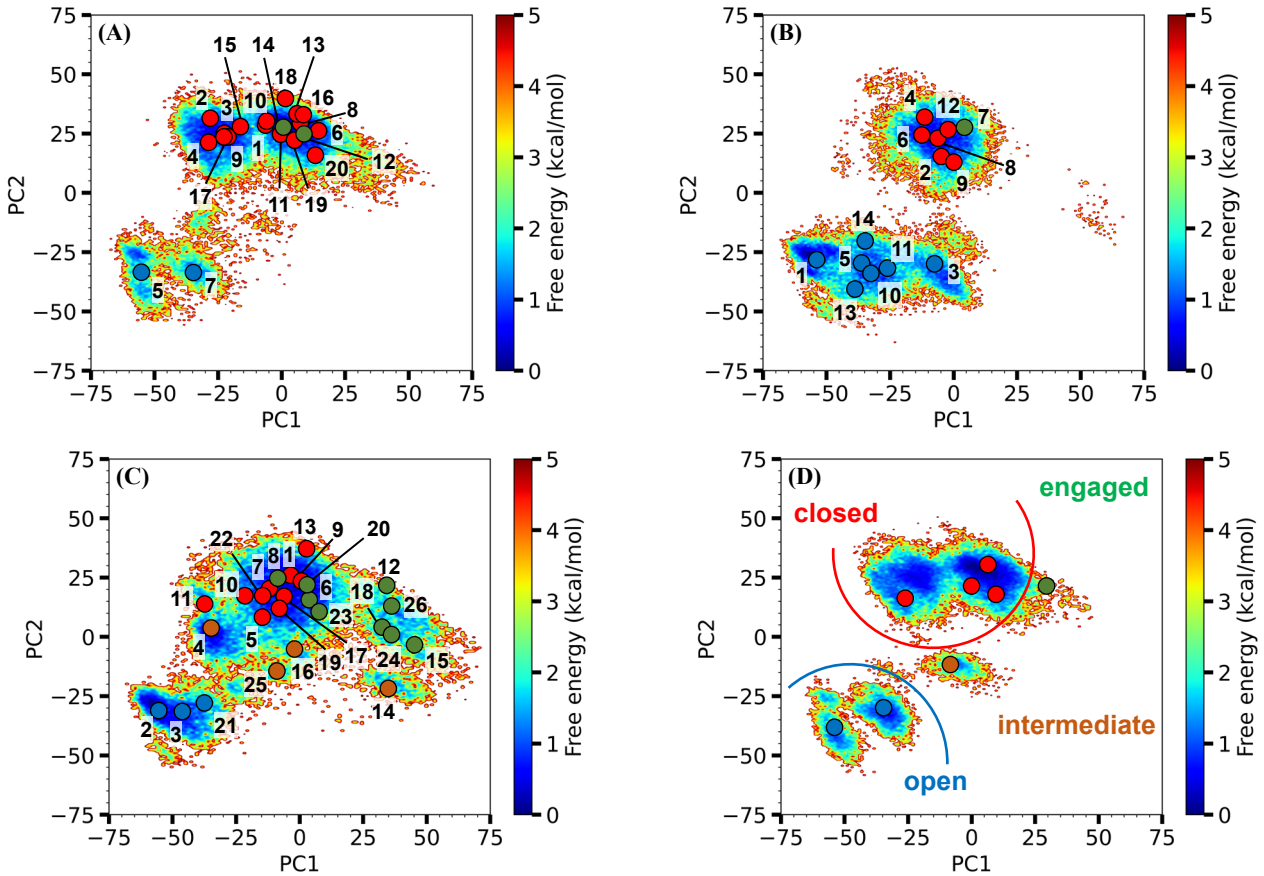

Figure 5 FEL of Cut190**SS and Cut190**SS_F77L configurations along the first and the second principal components (PC1 and PC2, respectively), with the contour value in kcal/mol. (A) Ca^{2+}-free Cut190**SS at 340 K. (B) Ca^{2+}-bound Cut190**SS at 340 K; the CA9 model, in which nine Ca^{2+} ions were added to the simulation box. (C) Ca^{2+}-free Cut190**SS_F77L at 340 K. The representative structures are also indicated by numbers and circles with the same color of respective forms. The representative structures have been submitted to the Biological Structure Model Archive (BSM-Arc), under BSM-00080 (doi:10.51093/bsm-00080). (D) Ca^{2+}-free Cut190**SS at 300 K. The locations of our experimental structures, open, closed, engaged, and intermediate forms, are indicated. PDB IDs of closed, open, and engaged forms are 7CTR, 5ZNO, and 5ZRR, respectively.

of Ca^{2+} was similar to that in the presence of Ca^{2+} under the reaction conditions used in this study. The catalytic activity of Cut190**SS_F77L at 70°C for both PBSA and PET was higher than that of Cut190**SS (Fig. 4), as observed for those at 37°C for PBSA reported previously [13].

The structural ensembles of Cut190**SS and Cut190**SS_F77L at 340 K were analyzed using McMD simulations. Figure 5 shows the first two principal components (PC1 and PC2, respectively) obtained via PCA to produce the FEL. A set of representative structures was obtained from the structural ensemble, and mapped onto the FEL. In the 2D landscape at 300 K, several islands were observed, which could be classified into open, closed, and engaged conformations, as determined by the crystal structures (Figs. 5D and 6). Notably, at 340 K, the FEL became more ragged, the respective islands partly merged in either the Ca^{2+}-bound state or the Ca^{2+}-unbound state, and the representative structures also merged (Figs. 5A-5C), indicating that the respective conformations were exchangeable. Therefore, catalytic activity was expressed even in the absence of Ca^{2+}. The population of the open conformation in the Ca^{2+}-bound state was relatively larger than that in the Ca^{2+}-unbound state (Figs. 5A and 5B), which was in good agreement with the crystal structure information showing that the Ca^{2+}-bound and Ca^{2+}-unbound structures of Cut190*SS are open and closed, respectively [6]. Our previous studies showed that Ca^{2+} releasing is needed for the conformational change from open to engaged forms [4,13]. The population of the conformational states of Cut190*SS would be changed from Fig. 5B to Fig. 5A by Ca^{2+} releasing. The respective islands of Cut190**SS_F77L were expanded more and merged than those of Cut190**SS (Figs. 5A and 5C), possibly correlating with differences in catalytic activity (Fig. 4).

Discussion

An enzyme expresses its catalytic activity by changing its structure or structural dynamics, some of which are regulated by metal-ion binding. Because the respective structures are located as potential energy minima in a folding funnel [25], the energy barriers between them must be overcome to change the structure from one to another [26]. Our crystal structure analyses of Cut190 mutants indicated that Ca^{2+} binding to Site 1 changed the structure from closed to open for substrate binding, followed by a conformational change to the engaged and ejecting forms (Fig. 6), along with substrate hydrolysis and product release [3-6,13]. Because proteins would crystallize from the most stable and populated structures, the major structure tends to be the crystal structure. Not only the major form of Cut190, but also the minor forms coexist in solution, and the population changes upon Ca^{2+} binding. Ca^{2+} binding can change the Cut190 structure to overcome the potential energy barriers between its respective forms. With increasing temperature, possibly because of the increased thermal fluctuation of the enzyme, the respective forms are exchangeable even in the absence of Ca^{2+}, resulting in the expression of catalytic activity. This was supported by McMD simulations, showing that the respective islands of the FEL observed at 300 K merged at 340 K (Fig. 5). At 300 K, the respective structures could be classified into open, closed, and engaged forms (Fig. 6). In contrast, at 340 K, closed and engaged forms were partially merged. The results also support the notion that the respective conformations were exchangeable, resulting in the catalytic activity even in the absence of Ca^{2+} (Fig. 4).

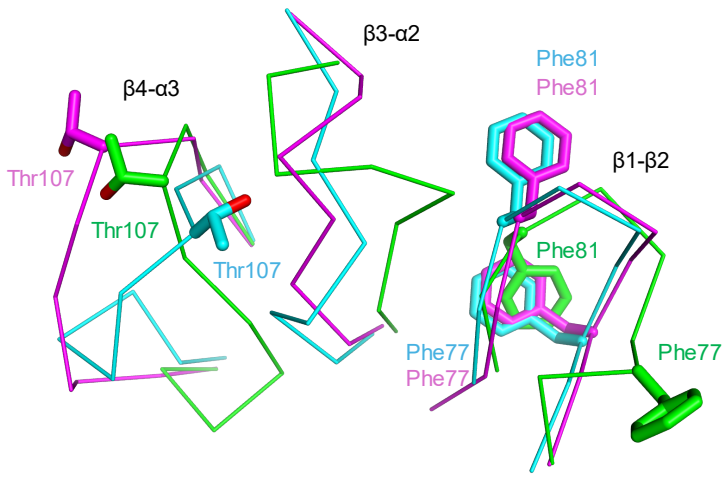

Figure 6 Local conformations of open (green, 5ZNO), closed (cyan, 7CTR), and engaged (purple, 5ZRR) forms of Cut190 mutants. These loop regions were used for the PCA analysis. Figure was prepared using the PYMOL software (https://www.pymol.org/).

We previously analyzed the binding thermodynamics of metal-ions to the inactive mutant of Cut190*, Cut190*S176A, using ITC [8]. The binding affinities and stoichiometries of Zn^{2+}, Mn^{2+}, and Mg^{2+} were also determined. As little heat was observed in the ITC for Ca^{2+} binding, the binding affinity of Ca^{2+} was lower than that of the other three metal-ions. Upon introduction of a disulfide-bond between residues 250 and 296, little heat was observed, even during Zn^{2+} binding (Fig. 3), as observed with respect to Cut190*SS [6]. While three Zn^{2+} molecules bound to Sites 1, 2, and 3 of Cut190*S176A with detectable ITC heat [8], all binding affinities decreased upon the introduction of a disulfide-bond. This further indicates that the introduction of a disulfide-bond at Site 2 could change the metal-ion binding properties not only at Site 2 but also at Sites 1 and 3. The Ca^{2+} binding affinities of Cut190 mutants with the disulfide-bonds would also decrease, based on the catalytic activities of Cut190* and Cut190**SS at 37°C, as described below. The catalytic activity of Cu190**SS in the presence of 0.25 mM Ca^{2+} was approximately 10%, which was slightly higher than the control without the enzyme (Fig. 4). In contrast, the catalytic activity of Cut190* in the presence of 0.25 mM Ca^{2+} was approximately 80% of that of 2.5 mM Ca^{2+} [7]. Taken together, the low activity of the disulfide-bond introduced mutants in the presence of 0.25 mM Ca^{2+} could be explained by the decreased Ca^{2+} binding affinity. As discussed previously [8,27], the weak binder Ca^{2+} would maintain enzyme fluctuations, and thus regulates enzyme function well. In contrast, the catalytic activity at 70°C in the presence of 0.25 mM Ca^{2+} was similar to those at higher Ca^{2+} concentrations (Fig. 4). Even in the absence of Ca^{2+}, the catalytic activity of PET at 70°C was similar to that in the presence of Ca^{2+}. These results are in good agreement with the McMD results, showing that the population of the closed form increased at 340 K. Furthermore, the potential energy barriers between the respective forms of enzyme would be lowered at 70°C where the enzyme can change the form even in the absence of Ca^{2+}. For PET degradation, it would be beneficial to use an enzyme without Ca^{2+}.

The increased stability and activity of Cut190**SS makes it a promising candidate for PET degradation. As shown in the chemical recycling of PET by engineered leaf-branch compost cutinase [10,11], the depolymerization of PET by enzymes around T_g is best for degrading the inner block of PET. Using Cut190**SS as a template, we are currently attempting to improve its catalytic activity for PET. Information on the structural dynamics obtained from McMD simulations will also contribute to the design of mutants with increased activity. The F77L mutation actually increased PET degradation [13]. We found that the F77L mutation increased the population of the closed and engaged forms at 300 K, which correlated well with the increased k_{cat} value of Cut190**SS_F77L (Table 2). Difference in structural dynamics between Cut190**SS and Cut190**SS_F77L in the absence or presence of Ca^{2+} was smaller than the detection limit of the present SEC-SAXS analysis (Fig. 2 and Table 1). McMD simulations for the population of the respective forms in solution showed that Ca^{2+} binding increased in the open form at 340 K (Fig. 5B), as well as at 300 K [13]. With increasing temperature, the boundaries of the respective FEL islands disappeared, indicating that the exchange between the respective forms became faster (Fig. 5). These results explain the catalytic activity of Cut190 regulated by Ca^{2+} binding and Ca^{2+} dependency decreasing with increasing temperature. These combined methods are useful not only for basic protein science to elucidate the structure-activity relationships, but also for the application of PET degradation and its chemical recycling.

Conclusions

The stabilized Cut190 mutants can degrade PET even in the absence of Ca^{2+} at 70°C. Multicanonical MD simulations showed that the conformational change of enzyme required for catalytic activity was induced upon Ca^{2+} binding and release at 37°C while that occurred even in the absence of Ca^{2+} with increasing temperature. The respective conformational states of Cut190 mutants correlated well with their catalytic activities.

Conflict of interest

The authors declare that they have no conflicts of interest with the contents of this article.

Author contributions

FK performed the experiment. NK and GJB performed the simulation. FK, NK, NN, and MO analyzed the data, and SN and HS contributed to the SAXS experiment. MO led the entire manuscript. All the authors reviewed the manuscript.

Data availability

The representative structures the raw simulation data, have been submitted to the Biological Structure Model Archive (BSM-Arc), under BSM-00080 (doi: 10.51093/bsm-00080).

Acknowledgements

The authors thank Emeritus Prof Fusako Kawai of Okayama University for providing the original plasmid of Cut190 based on the license agreement. This study was supported by Nanken-Kyoten, Science Tokyo, the Collaborative Research Program of Institute for Protein Research, Osaka University, CR-22-05, CR-23-02 and CR-24-02, and Japan Agency for Medical Research and Development (AMED) (24ae0121028h0004). Computational resources of the TSUBAME3.0 and TSUBAME4.0 systems (Institute of Science Tokyo) were provided by the HPCI Research Project (hp210002, hp220002, hp230003, hp240005 and hp240121). The SEC-SAXS experiments at the synchrotron radiation facility were performed at the BL38B1 of SPring-8 with the approval of JASRI (Proposal No. 2023A2529, 2023B2524, 2023B2728, and 2024A2524). This study was supported by the Grand-in-Aid for Scientific Research from the Japan Society for the Promotion of Science, JP21H02120 and JP24K09339.

References

[1] Nyyssölä, A. Which properties of cutinases are important for applications? Appl. Microbiol. Biotechnol. 99, 4931–4942 (2015). https://doi.org/10.1007/s00253-015-6596-z

[2] Kawai, F., Oda, M., Tamashiro, T., Waku, T., Tanaka, N., Yamamoto, M., et al. A novel Ca^{2+}-activated, thermostabilized polyesterase capable of hydrolyzing polyethylene terephthalate from *Saccharomonospora viridis* AHK190. Appl. Microbiol. Biotechnol. 98, 10053–10064 (2014). https://doi.org/10.1007/s00253-014-5860-y

[3] Miyakawa, T., Mizushima, H., Ohtsuka, J., Oda, M., Kawai, F., Tanokura, M. Structural basis for the Ca^{2+}-enhanced thermostability and activity of PET-degrading cutinase from *Saccharomonospora viridis* AHK190. Appl. Microbiol. Biotech. 99, 4297–4307 (2015). https://doi.org/10.1007/s00253-014-6272-8

[4] Numoto, N., Kamiya, N., Bekker, G. -J., Yamagami, Y., Inaba, S., Ishii, K., et al. Structural dynamics of PET-degrading cutinase-like enzyme from *Saccharomonospora viridis* AHK190 in substrate-bound states elucidates Ca^{2+} driven catalytic cycle. Biochemistry 57, 5289–5300 (2018). https://doi.org/10.1021/acs.biochem.8b00624

[5] Senga, A., Numoto, N., Yamashita, M., Iida, A., Ito, N., Kawai, F., et al. Multiple structural states of Ca^{2+} regulated PET hydrolase, Cut190, and its correlation with activity and stability. J. Biochem. 169, 207–213 (2021). https://doi.org/10.1093/jb/mvaa102

[6] Emori, M., Numoto, N., Senga, A., Bekker, G. -J., Kamiya, N., Kobayashi, Y., et al. Structural basis of mutants of PET-degrading enzyme from *Saccharomonospora viridis* AHK190 with high activity and thermal stability. Proteins 89, 502–511 (2021). https://doi.org/10.1002/prot.26034

[7] Oda, M., Yamagami, Y., Inaba, S., Oida, I., Yamamoto, M., Kitajima, S., et al. Enzymatic hydrolysis of PET: Functional roles of three Ca^{2+} ions bound to a cutinase-like enzyme, Cut190*, and its engineering for improved activity. Appl. Microbiol. Biotechnol. 102, 10067–10077 (2018). https://doi.org/10.1007/s00253-018-9374-x

[8] Senga, A., Hantani, Y., Bekker, G. -J., Kamiya, N., Kimura, Y., Kawai, F., et al. Metal binding to cutinase-like enzyme from *Saccharomonospora viridis* AHK190 and its effects on enzyme activity and stability. J. Biochem. 166, 149–156 (2019). https://doi.org/10.1093/jb/mvz020

[9] Oda, M. Structural basis for Ca^{2+}-dependent catalysis of a cutinase-like enzyme and its engineering: application to enzymatic PET depolymerization. Biophys. Physicobiol. 18, 168–176 (2021). https://doi.org/10.2142/biophysico.bppb-v18.018

[10] Tournier, V., Topham, C. M., Gilles, A., David, B., Folgoas, C., Moya-Leclair, E., et al. An engineered PET depolymerase to break down and recycle plastic bottles. Nature 580, 216–219 (2020). https://doi.org/10.1038/s41586-020-2149-4

[11] Tournier, V, Duquesne, S, Guillamot, F, Cramail, H, Taton, D, Marty, A, et al. Enzymes' power for plastics degradation. Chem. Rev. 123, 5612–5701 (2023). https://doi.org/10.1021/acs.chemrev.2c00644

[12] Kawai, F., Kawabata, T., Oda, M. Current state and perspectives related to the polyethylene terephthalate hydrolases available for biorecycling. ACS Sustainable Chem. Eng. 8, 8894–8908 (2020). https://doi.org/10.1021/acssuschemeng.0c01638

[13] Numoto, N., Kondo, F., Bekker, G., -J., Liao, Z., Yamashita, M., Iida, A., et al. Structural dynamics of the Ca^{2+}-regulated cutinase towards structure-based improvement of PET degradation activity. Int. J. Biol. Macromol. 281, 136597 (2024). https://doi.org/10.1016/j.ijbiomac.2024.136597

[14] Higo, J., Ikebe, J., Kamiya, N., Nakamura, H. Enhanced and effective conformational sampling of protein molecular systems for their free energy landscapes. Biophys. Rev. 4, 27–44 (2012). https://doi.org/10.1007/s12551-011-0063-6

[15] Kitao, A., Hirata, F., Gō, N. The effects of solvent on the conformation and the collective motions of protein: Normal mode analysis and molecular dynamics simulations of melittin in water and in vacuum. Chem. Phys. 158, 447–472 (1991). https://doi.org/10.1016/0301-0104(91)87082-7

[16] Kamiya, N., Higo, J., Nakamura, H. Conformational transition states of a β-hairpin peptide between the ordered and disordered conformations in explicit water. Protein Sci. 11, 2297–2307 (2002). https://doi.org/10.1110/ps.0213102
[17] Bekker, G. -J., Kamiya, N. Dynamic docking using multicanonical molecular dynamics: Simulating complex formation at the atomistic level. Methods Mol. Biol. 2266, 187–202 (2021). https://doi.org/10.1007/978-1-0716-1209-5_11
[18] Bekker, G. -J., Kamiya, N. Advancing the field of computational drug design using multicanonical molecular dynamics-based dynamic docking. Biophys. Rev. 14, 1349–1358 (2022). https://doi.org/10.1007/s12551-022-01010-z
[19] Bekker, G. -J., Araki, M., Oshima, K., Okuno, Y., Kamiya, N. Dynamic docking of a medium-sized molecule to its receptor by multicanonical MD simulations. J. Phys. Chem. B 123, 2479–2490 (2019). https://doi.org/10.1021/acs.jpcb.8b12419
[20] Yoshida, M., Hanazono, Y., Numoto, N., Nagao, S., Yabuno, S., Kitagawa, Y., et al. Affinity-matured antibody with a disulfide bond in H-CDR3 loop. Arch. Biochem. Biophys. 758, 110068 (2024). https://doi.org/10.1016/j.abb.2024.110068
[21] Shimizu, N., Yatabe, K., Nagatani, Y., Saijyo, S., Kosuge, T., Igarashi, N. Software development for analysis of small-angle X-ray scattering data. AIP Conf. Proc. 1741, 050017 (2016). https://doi.org/10.1063/1.4952937
[22] Yonezawa, K., Takahashi, M., Yatabe, K., Nagatani, Y., Shimizu, N. MOLASS: Software for automatic processing of matrix data obtained from small-angle X-ray scattering and UV-visible spectroscopy combined with size-exclusion chromatography. Biophys. Physicobiol. 20, e200001 (2023). https://doi.org/10.2142/biophysico.bppb-v20.0001
[23] Svergun, D. I. Determination of the regularization parameter in indirect-transform methods using perceptual criteria. J. Appl. Crystallogr. 25, 495–503 (1992). https://doi.org/10.1107/S0021889892001663
[24] Manalastas-Cantos, K., Konarev, P. V., Hajizadeh, N. R., Kikhney, A. G., Petoukhov, M. V., Molodenskiy, D. S., et al. ATSAS 3.0: Expanded functionality and new tools for small-angle scattering data analysis. J. Appl. Crystallogr. 54, 343–355 (2021). https://doi.org/10.1107/S1600576720013412
[25] Nassar, R., Dignon, G. L., Razban, R. M., Dill, K. A. The protein folding problem: The role of theory. J. Mol. Biol. 433, 167126 (2021). https://doi.org/10.1016/j.jmb.2021.167126
[26] Du, S., Kretsch, R. C., Parres-Gold, J., Pieri, E., Cruzeiro, V. W. D., Zhu, M., et al. Conformational ensembles reveal the origins of serine protease catalysis. Science 387, 735 (2025). https://doi.org/10.1126/science.ado5068
[27] Inaba, S., Kamiya, N., Bekker, G. -J., Kawai, F., Oda, M. Folding thermodynamics of PET-hydrolyzing enzyme Cut190 depending on Ca^{2+} concentration. J. Therm. Anal. Calorim. 135, 2655–2663 (2019). https://doi.org/10.1007/s10973-018-7447-9

This article is licensed under the Creative Commons Attribution-NonCommercial-ShareAlike 4.0 International License.
To view a copy of this license, visit https://creativecommons.org/licenses/by-nc-sa/4.0/.